7.2 ESTIMATION OF HELIUM PRODUCTION BY THE NICKEL FOIL IMPLANTER TECHNIQUE FOR BEND STRESS RELAXATION TESTS IN THE TITAN PHASE II RABBIT IRRADIATION CAMPAIGN

—K. Ozawa, Y. Katoh, L.L. Snead (Oak Ridge National Laboratory), T. Yamamoto (University of California, Santa Barbara), T. Hinoki (Kyoto University), A. Hasegawa (Tohoku University)

OBJECTIVE

This report aims to estimate helium production in the bend stress relaxation test specimens by the nickel foil implanter technique, used in the Phase II campaign of the US-Japan Joint Research TITAN Project.

SUMMARY

He profiles in bend stress relaxation specimens from the thin Ni foil implanter technique were calculated for the TITAN Phase II Campaign. The calculations revealed that the distribution of the implanted transmuted helium is uniform at 2.1, 15 and 21 appm He/dpa to a depth of 11 μm for the case of a 2 μm-thick implanter foil for irradiation to 1, 10 and 20 $\times 10^{25}$ n/m^2 (E > 0.1 MeV), equivalent to 1, 10, and 20 dpa-SiC in the HFIR-PTP. It is noted that the He/dpa ratio is strongly fluence dependent, since natural Ni was used for the implanter foil and hence the He is produced by a two neutron capture sequence.

PROGRESS AND STATUS

Introduction

In the TITAN Phase I irradiation campaign, transient irradiation creep properties of silicon carbide (SiC) have been investigated and engineering important experimental results have been revealed about stress exponent (n = 1), linear swelling-creep relationship, and effects of microstructural features such as grain size, grain boundary and crystal structure on irradiation creep [1]. Subsequently, a Phase II irradiation campaign is planned and this focuses on both steady-state irradiation enhanced creep and helium effects for relatively high dose conditions, in order to understand the whole irradiation creep phenomena.

Regarding He effect study, ingenuity is required to simulate fusion relevant He production in fission reactor neutron irradiation experiments, because the neutron spectrum is completely different from 14 MeV fusion spectrum and He production is generally low. For He effects studies of SiC using neutron irradiation, some researchers have used boron-sintered SiC to simulate fusion, since B has a large (n,α) cross section and is easily transmuted to He by nuclear reaction. However, the physical properties of SiC have been totally changed by B assisted sintering and the helium production was not estimated precisely and quantitatively.

One of the solutions for these issues is foil implanter technique, which utilizes ^{59}Ni(n,α) nuclear reaction to inject transmuted He to a specimen from a Ni foil attached on it. The base concept has been originally derived by Gould [2], and suggested for the fusion study by Odette [3]. In practical, the He flow property of the fusion relevant alloys in the HFIR irradiations (JP-26, -27 and -28/29 campaigns) was reported by Yamamoto et al. [4].

This report aims to estimate He production in the bend stress relaxation (BSR) test specimens by nickel foil implanter technique, associated with the Phase II campaign in the US-Japan Joint Research Project.

Table I. Test matrix for the TITAN Phase 2 Campaign. Only the specimens related to this report have been excerpted. Other monolithic SiC, SiC/SiC composites and advanced SiC fibers without Ni foils will be irradiated at the same time. (This table continues on the next page.)

Capsule ID	Irrad. Temp.	DPA	Unit ID	Curv. [mm]	Mat.	Thick. [μm]	Initial Stress [MPa]	Note
T10-01J	300	1	21P3	R 200	RH	50	56	
					RH	50	56	(i)
					Ni	2	-	
					RH	50	56	(ii)
					Ni	2	-	
					RH	50	56	(iii)
					RH	100	113	
					RH	100	113	
					RH	150	169	
					RH	150	169	
					CT	50	56	(i)
					Ni	2	-	
					CT	50	56	(ii)
					Ni	2	-	
					CT	50	56	(iii)
T10-02J	300	10	22P3	R 100	RH	50	113	
					RH	50	113	(i)
					Ni	2	-	
					RH	50	113	(ii)
					Ni	2	-	
					RH	50	113	(iii)
					RH	100	225	
					RH	100	225	
					RH	150	338	
					RH	150	338	
					CT	50	113	(i)
					Ni	2	-	
					CT	50	113	(ii)
					Ni	2	-	
					CT	50	113	(iii)
T10-03J	300	20	23P3	R100	RH	50	113	
					RH	50	113	(i)
					Ni	2	-	
					RH	50	113	(ii)
					Ni	2	-	
					RH	50	113	(iii)
					RH	100	225	
					RH	100	225	
					RH	150	338	
					RH	150	338	
					CT	50	113	(i)
					Ni	2	-	
					CT	50	113	(ii)
					Ni	2	-	
					CT	50	113	(iii)
T10-04J	500	10	24P3	R100	RH	50	113	
					RH	50	113	(i)
					Ni	2	-	
					RH	50	113	(ii)
					Ni	2	-	
					RH	50	113	(iii)
					RH	100	225	
					RH	100	225	

					RH	150	338	
					RH	150	338	
					CT	50	113	(i)
					Ni	2	-	
					CT	50	113	(ii)
					Ni	2	-	
					CT	50	113	(iii)
T10-05J	500	20	25P3	R100	RH	50	113	
					RH	50	113	(i)
					Ni	2	-	
					RH	50	113	(ii)
					Ni	2	-	
					RH	50	113	(iii)
					RH	100	225	
					RH	100	225	
					RH	150	338	
					RH	150	338	
					CT	50	113	(i)
					Ni	2	-	
					CT	50	113	(ii)
					Ni	2	-	
					CT	50	113	(iii)
T10-06J	800	10	26P3	R100	RH	50	113	
					RH	50	113	(iv)
					RH	50	113	(iv)
					RH	50	113	(iv)
					RH	100	225	
					RH	150	338	
					RH	150	338	
					CT	50	113	(iv)
					CT	50	113	(iv)
					CT	50	113	(iv)
T10-07J	800	20	27P3	R100	RH	50	113	
					RH	50	113	(iv)
					RH	50	113	(iv)
					RH	50	113	(iv)
					RH	100	225	
					RH	100	225	
					RH	150	338	
					RH	150	338	
					CT	50	113	(iv)
					CT	50	113	(iv)
					CT	50	113	(iv)
T10-08J	1200	10	28P3	R100	RH	50	113	
					RH	50	113	(iv)
					RH	50	113	(iv)
					RH	50	113	(iv)
					RH	100	225	
					RH	100	225	
					RH	150	338	
					CT	50	113	(iv)
					CT	50	113	(iv)
					CT	50	113	(iv)

Irrad. Temp.: Irradiation temperature, Curv.: radius of curvature of the fixture, Mat.: material, RH: Roam & Haas CVD-SiC, CT: CoorsTek CVD-SiC, Ni: Ni foil for implanter, Thick.: specimen thickness. (i) He on the compression side. (ii) He on both tension and compression sides. (iii) He on the tension side. (iv) No He effect.

Materials and Specimen Loading

The test matrix for this irradiation plan is listed in Table I. Chemically vapor deposited (CVD) monolithic silicon carbide (SiC) manufactured by Roam & Haas and CoorsTek with thickness of 50-200 μm were used. It is noted that only specimens related to this report have been excerpted. Other SiC materials (CVD-SiC by Roam & Haas and CoorsTek, single crystal 6H-SiC by Cree, and SiC/SiC composites processed by nano infiltration method) and advanced SiC fibers (Hi-Nicalon™ Type-S, Tyranno™-SA3, experimental Sylramic™ and experimental Sylramic™-iBN) without Ni foils will be irradiated at the same time. The details of the full test matrix are given elsewhere [5].

Consideration of appropriate nuclei for achieving (n,α) reactions with high energy, radiation activity of specimens after neutron irradiation, and machinability of a implanter foil, led to selection of 2 μm-thick nickel foils manufactured by Goodfellow Cambridge Limited (Huntingdon, England). The purity of Ni in the foil is 99.95% and other major impurities are given in the manufacturer's catalogue [6]. The Ni foils, specimens and fixtures are shown in Figure 1. The Ni foils were cut with a fine wire saw to 40 × 1 × 0.002 mm and were located adjacent to the SiC specimen using water lubrication when loading the specimen holders for the irradiation experiment.

Neutron irradiation to 1, 10, 20 dpa-SiC at 300-1200°C is planned, as shown in Table I. However, Ni foils were not used with the specimens to be irradiated at 800, 1000 and 1200°C, since a strong interaction between Si and Ni is a concern. For example, it has been reported that reaction layer between SiC and Ni was formed when annealed above 800°C [7].

The initial stage bend stress (σ) was calculated by the following simple equation,

$$\sigma = \varepsilon E = \frac{t}{2R} E \tag{1}$$

where ε is the strain, E the elastic modulus, t the specimen thickness and R the radius of curvature of the fixture. The Young's modulus of CVD-SiC was assumed to be 450 GPa. A more complete description of the BSR experimental technique is given elsewhere [8].

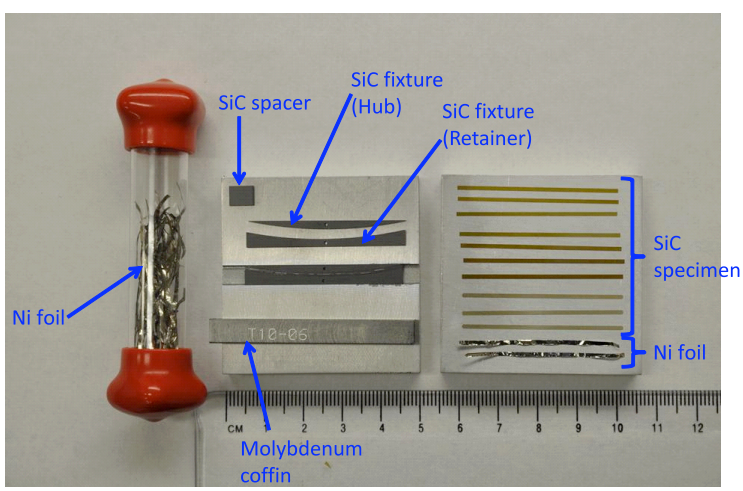

Figure 1. Specimens, Ni foils and SiC fixtures.

Analysis

He Production of the Ni foil [9]

He is transmuted from Ni through the following ^{58}Ni(n,γ)^{59}Ni(n,α)^{56}Fe reactions;

$$^{58}_{28}\text{Ni} + ^{1}_{0}\text{n} \rightarrow ^{59}_{28}\text{Ni} + 9.00\ \text{MeV}\ (\gamma\ \text{decay}) \tag{2}$$

$$^{59}_{28}\text{Ni} + ^{1}_{0}\text{n} \rightarrow ^{56}_{26}\text{Fe} + ^{4}_{2}\text{He} + 5.09\ \text{MeV} \tag{3}$$

The energy of α-particles from this reaction sequence is 5.09 × 4/(56+4) = 4.75 [MeV]. The production of helium (i.e. He concentration in the foil: C_f) from nickel by the sequential nuclear reactions with this energy is calculated as follows,

$$C_f = \frac{N(He)}{N_0(^{58}Ni)} = \frac{\sigma_\alpha[\sigma_T(1-\exp(-\sigma_\gamma\phi t)) - \sigma_\gamma(1-\exp(-\sigma_T\phi t))]}{\sigma_T(\sigma_T - \sigma_\gamma)} \tag{4}$$

Where

$N(He)$	= Helium atoms produced at time t
$N_0(^{58}Ni)$	= Initial number of ^{58}Ni atoms
σ_α	= ^{59}Ni(n,α) cross section
σ_T	= ^{59}Ni total absorption cross section
σ_γ	= ^{58}Ni(n,γ) cross section
ϕ	= Total flux
t	= Irradiation time

All cross sections should be averaged over the neutron energy spectrum. Total helium production from nickel includes not only the low-energy production given in Eq. (3), but also fast neutron production from both ^{58}Ni and ^{60}Ni. However, the helium production by fast neutrons was ignored in this estimation because the contribution to the total helium production seems to be very small (<0.05%). Figure 2 shows the calculated result for He production by this calculation, plotted against total neutron fluence. Parameters used were listed in Table II. It is noted that the cross section values in the HFIR Peripheral Target Position (PTP) in the CTR-32 campaign [9] were used in the calculation.

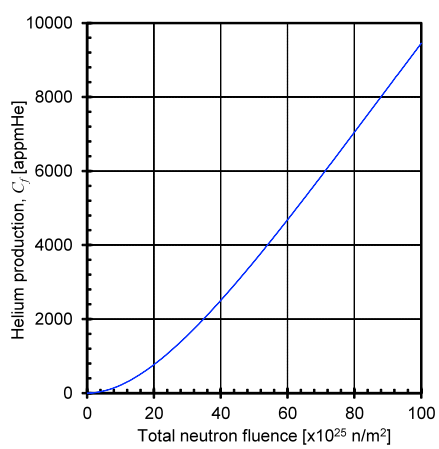

Figure 2. Calculated result of He production plotted against total neutron fluence in the HFIR-PTP.

Table II. Parameters used in the Ni foil implanter design in this study. Subscript f and S denote "foil" and "specimen."

Symbol	Description	Value	Unit	Ref.
σ_α	Spectral averaged ^{59}Ni(n,α) cross section	4.33	b (×10^{-28} m^2)	[9]
σ_T	Spectral averaged ^{59}Ni total absorption cross section	34.29	b (×10^{-28} m^2)	[9]
σ_γ	Spectral averaged ^{58}Ni(n,γ) cross section	1.63	b (×10^{-28} m^2)	[9]
$^{58}Ni/^{Tot}Ni$	Relative isotopic abundance of ^{58}Ni	0.683	-	[10]
E_{He}	^{4}He nucleation energy	4.75	MeV	
R_f (R_{Ni})	Helium injection average range for Ni	8.66	μm	[11]
R_S (R_{SiC})	Helium injection average range for SiC	14.6	μm	[11]
d_f (d_{Ni})	Density of Ni	8.91	g/cm^3	-
d_S (d_{SiC})	Density of SiC	3.21	g/cm^3	-
M_f (M_{Ni})	Atomic mass of Ni	58.69	g/mol	-
M_S (M_{SiC})	Atomic mass of SiC	41.4	g/mol	-
ρ_f (ρ_{Ni})	Molar density of Ni	0.152	g-atom/cm^3	-
ρ_S (ρ_{SiC})	Molar density of SiC	0.155	g-atom/cm^3	-
$\phi't/\phi t$	Ratio of thermal (E < 0.5 eV) to total neutron fluence	0.414	-	[12]
$\phi''t/\phi t$	Ratio of fast (E > 0.1 MeV) to total neutron fluence	0.268	-	[12]

He Implantation Profiles [4]

The ^{59}Ni isotope in the implanter foil produces an α-particle with characteristic energy and corresponding range in the foil and sample of R_f and R_S, respectively. Assume that the foil thickness is larger than the implanted He range in the specimen, as shown in Figure 3a (thick foil case). The α-particles emitted from the foil under neutron irradiation are implanted in the specimen to the depth of R_S. All calculations in this section assume the area (y, z) dimensions of the implanter foil-specimen are much larger than R_f, hence, edge effects can be neglected. For simplicity, first assume $R_f = R_S = R$ and ignore α-particle straggling. The He concentration, C_{He}, at a depth x ($x < R$) in the specimen should be proportional to the area fraction, $f(x)$, of the spherical shell in the implanter foil of radius, R, centered on x, as shown in Figure 4. The $f(x)$ is expressed as;

$$f(x) = \int_0^{\theta_{\max}} 2\pi R \sin\theta \, R d\theta \Big/ 4\pi R^2 = \frac{1}{2}\left(1 - \frac{x}{R}\right) \tag{5}$$

where θ is the angle between the radial vector R and the normal to the specimen surface and θ_{max} occurs at the implanter foil/specimen boundary. The resulting He concentration profile is linear with $f(x)$ decreasing from 1/2 at x = 0 to 0 at $x = R_S$. Therefore the He concentration in the specimen (C_{He}) can be described as follows:

$$C_{He}(x) = \frac{C_f}{2}\frac{\rho_f}{\rho_S}\frac{R_f}{R_S}\left(1 - \frac{x}{R_S}\right) \tag{6}$$

where

C_f = volumetric concentration of He in the implanter foil which is the same as the bulk concentration for a given implanter foil composition and neutron dose (The

corresponding molar (or atomic) concentration c_f must be adjusted by multiplying C_f by the ration of the foil/specimen atomic densities (N), N_f/N_S).

R_f, R_S = Helium injection average range for the foil and specimen, respectively, calculated using TRIM-98 code as the average of 99999 4.75 MeV He ions [11].

ρ_f, ρ_S = molar density of the foil and the specimen, respectively.

It is noted that both differences 1) in the α-particle ranges between the foil and the specimen (R_f and R_S), and 2) in the molar densities (ρ_f and ρ_S), should be accounted for by ratio factors of R_f/R_S and ρ_f/ρ_S. In summary, the schematic illustration of the He distribution for the thick foil case was shown in Figure 3b.

Using the result of the thick foil case described above, the result for the thin foil case ($t_f < R_S$, shown in Figure 3c), can be calculated. The profile of the thin foil case (red bold line in Figure 3d) could be simply obtained by subtracting the missing contribution from the (n,α) reactions further from the interface (blue dotted line), from the thick-foil profile (black solid line). Therefore, in the thin foil case where $R_f \neq R_S$ and $x_m = R_f(1-t_f/R_S)$, the He concentration vs. position x can be described as follows:

$$C_{He}(x) = \begin{cases} \dfrac{C_f}{2}\dfrac{\rho_f}{\rho_S}\dfrac{t_f}{R_S} & : 0 < x < R_S(1 - t_f / R_f) \\ \dfrac{C_f}{2}\dfrac{\rho_f}{\rho_S}\dfrac{R_f}{R_S}\left(1 - \dfrac{x}{R_S}\right) & : R_S(1 - t_f / R_f) < x < R_S \\ 0 & : R_S < x \end{cases} \quad (7)$$

Results

Figure 5 illustrates the calculated results for neutron irradiation to 1, 10 and 20 dpa-SiC at the HFIR PTP with different Ni foil thickness (t_f = 1, 2, 3 and 8.66 μm). In this calculation, 1 dpa-SiC = 1 × 10^{25} n/m^2 (E > 0.1 MeV) = 3.74 x 10^{25} n/m^2 (total fluence), is assumed. This assumption is based on Ref. [12], but similar ratios of thermal or fast to total fluence at the target positions is confirmed (Table III). The calculations show that a uniform He/dpa ratio of 2.1, 15 and 21 appm/dpa is achieved to a depth of x_m = 11 μm for the case of t_f = 2 μm with 1, 10 and 20 dpa irradiation. When x_m is greater than 11 μm, the ratio decreased proportionally with x, resulting in C_{He} = 0 at x = 14.5 μm. It is noted that the He/dpa ratio is strongly fluence dependent, since natural Ni was used for the implanter foil and hence the He is produced by a two neutron capture sequence.

Table III. Neutron fluence at the HFIR target positions in previous irradiation experiments, calculated by Greenwood et al. [12-15]

Campaign	Position	Cycles	Neutron Fluence [×10^{22} n/cm^2]					Ratio		Ref.
			Total	Thermal < 0.5 eV	0.5 eV - 0.1 MeV	Fast > 0.1 MeV	> 1 MeV	Thermal /Total	Fast /Total	
JP-23	Target, G6	322-326	4.39	1.92	1.36	1.12	0.565	0.437	0.255	[13]
JP-9, 12, 15	Target	289-324	26.3	10.9	8.39	7.06	3.67	**0.414**	**0.268**	[12]
JP-20	Target	322-326	4.19	1.84	1.32	1.05	0.519	0.439	0.251	[14]
CTR-62, 63	Target	335-341	6.91	3.15	2.08	1.68	0.85	0.456	0.243	[15]

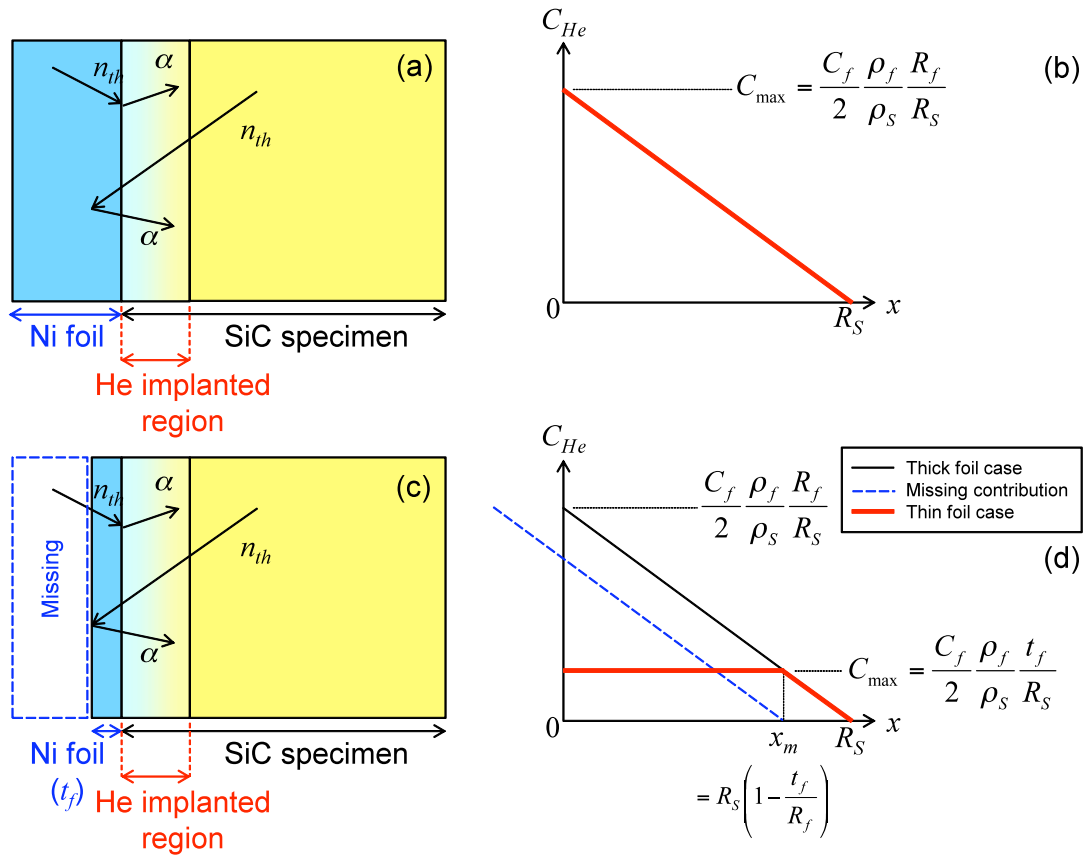

Figure 3. Schematic illustration of Ni foil implanter concept from one side of a specimen: (a) Thick foil case, where the foil thickness is larger than the He implanted average range. (b) He profile for the thick foil case. (c) Thin foil case, where the thickness is smaller than the He range. (d) He profile for the thin foil case.

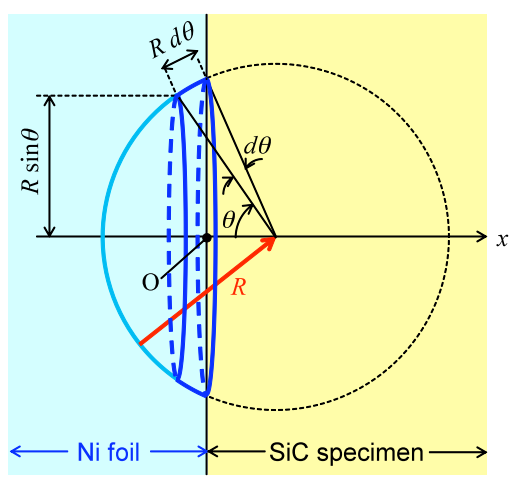

Figure 4. The implanter source volume for He deposited at a depth x in the specimen.

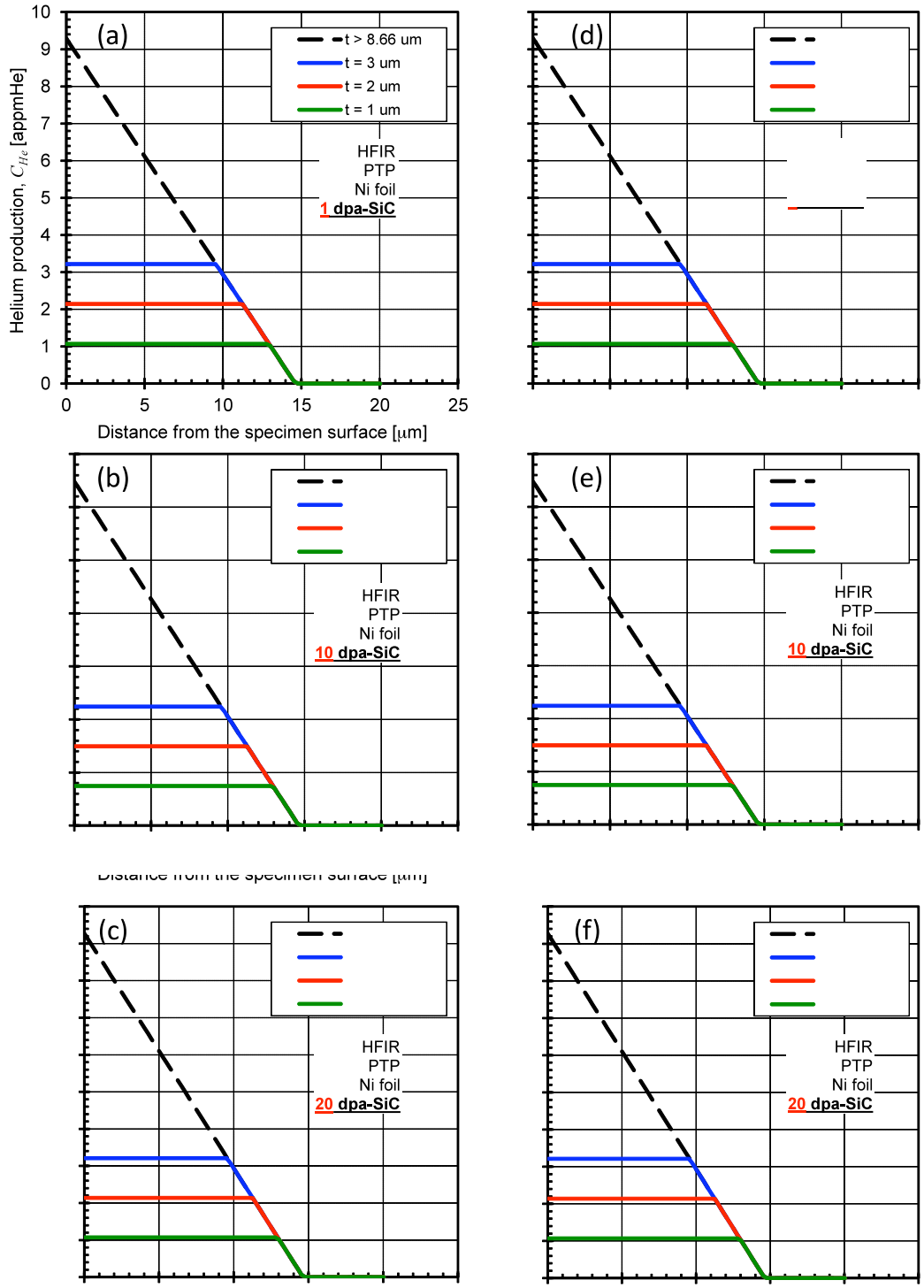

Figure 5. He production profiles in SiC specimens for (a) 1, (b) 10 and (c) 20 dpa conditions corresponding HFIR Target 2 position, respectively for Ni implanter foils with t_f = 1, 2, 3 and 8.66 μm. The corresponding He/dpa ratios are also plotted in (d)-(f).

Acknowledgement

This research is sponsored by the Office of Fusion Energy Sciences, US Department of Energy under contract DE-AC05-00OR22725 with UT-Battelle, LLC, and also a part TITAN US Department of Energy/Japanese Ministry of Education, Culture, Sports, Science and Technology (MEXT) collaboration for fusion material system research. Irradiation will be conducted in the Department of Energy High Flux Isotope Reactor User Facility starting in February 2011.

References

[1] Y. Katoh, L.L. Snead, A. Hasegawa, S. Nogami, T. Hinoki, Y.B. Choi, "Irradiation Creep in Silicon Carbide: Experimental Results from TITAN Program and Implications to Stress Evolution in Flow Channel Inserts for Fusion Liquid Metal Blankets," ANS 19th Topical Meeting on the Technology of Fusion Energy (TOFE-19), November 7-11 2010, Riviera Hotel, Las Vegas, Nevada, USA.
[2] T.H. Gould and W.R. McConnell, Proc. Int. Conf. on Radiation Effects and Tritium Technology for Fusion Reactors, Gatlingburg, TN, Oct. 1975, CONF-750989, V2 (1976) 387.
[3] G.R. Odette, J. Nucl. Mater. 141-143 (1986) 1011.
[4] T. Yamamoto, G.R. Odette, L.R. Greenwood, Fusion Mater. DOE/ER-0313/38 (2005) 95.
[5] Y. Katoh, et al., Fusion Mater. DOE/ER-0313/49 (2011), this report.
[6] http://www.goodfellow.com/pdf/4728_1111010.pdf
[7] J.H. Culpen, A.A. Kodentsov, J.J. van Loo, Z. Metallkd. 86 (1995) 8.
[8] Y. Katoh, L.L. Snead, Ceram. Eng. Sci. Proc. 26 (2005) 265
[9] L.R. Greenwood, D.W. Kneff, R.P. Skowronski, F.M. Mann, J. Nucl. Mater. 123 (1984) 1002.
[10] L.R. Greenwood, J. Nucl. Mater. 115 (1983) 137.
[11] According to the TRIM-98 code: J.F. Ziegler, J.P. Biersack, U. Littmark, "The Stopping and Range of Ions in Solids," Pergamon Press, 109 (1985).
[12] L.R. Greenwood, C.A. Baldwin, Fusion Mater. DOE/ER-0313/23 (1997) 301.
[13] L.R. Greenwood, R.T. Ratner, Fusion Mater. DOE/ER-0313/21 (1996) 229.
[14] L.R. Greenwood, C.A. Baldwin, Fusion Mater. DOE/ER-0313/23 (1997) 305.
[15] L.R. Greenwood, C.A. Baldwin, Fusion Mater. DOE/ER-0313/26 (1999) 199.